frontiers in Earth Science

ORIGINAL RESEARCH
published: 19 November 2021
doi: 10.3389/feart.2021.723382

The Ice-Rich Permafrost Sequences as a Paleoenvironmental Archive for the Kara Sea Region (Western Arctic)

I. D. Streletskaya[1], A. A. Pismeniuk[1,2], A. A. Vasiliev[3,4], E. A. Gusev[2], G. E. Oblogov[3,4] and N. A. Zadorozhnaya[3]*

[1]Faculty of Geography, Lomonosov Moscow State University, Moscow, Russia, [2]All-Russia Institute for Geology and Mineral Resources of the World Ocean (VNIIOkeangeologia), Saint Petersburg, Russia, [3]Earth Cryosphere Institute of Tyumen Scientific Centre SB RAS, Tyumen, Russia, [4]Tyumen State University, Tyumen, Russia

The Kara Sea coast and part of the shelf are characterized by wide presence of the ice-rich permafrost sequences containing massive tabular ground ice (MTGI) and ice wedges (IW). The investigations of distribution, morphology and isotopic composition of MTGI and IW allows paleoenvironmental reconstructions for Late Pleistocene and Holocene period in the Kara Sea Region. This work summarizes result of long-term research of ice-rich permafrost at eight key sites located in the Yamal, Gydan, Taimyr Peninsulas, and Sibiryakov Island. We identified several types of ground ice in the coastal sediments and summarized data on their isotopic and geochemical composition, and methane content. We summarized the available data on particle size distribution, ice chemical composition, including organic carbon content, and age of the enclosing ice sediments. The results show that Quaternary sediments of the region accumulated during MIS 5 – MIS 1 and generally consisted of two main stratigraphic parts. Ice-rich polygenetic continental sediments with syngenetic and epigenetic IW represent the upper part of geological sections (10–15 m). The IW formed in two stages: in the Late Pleistocene (MIS 3 – MIS 2) and in the Holocene cold periods. Oxygen isotope composition of IW formed during MIS 3 – MIS 2 is on average 6‰ lower than that of the Holocene IW. The saline clay with rare sand layers of the lower part of geological sections, formed in marine and shallow shelf anaerobic conditions. MTGI present in the lower part of the sections. The MTGI formed under epigenetic freezing of marine sediments immediately after sea regression and syngenetic freezing of marine sediments in the tidal zone and in the conditions of shallow sea.

Keywords: permafrost, massive tabular ground ice, ice wedges, Kara Sea coast, stable isotope, paleogeography

OPEN ACCESS

Edited by:
Duane Froese,
University of Alberta, Canada

Reviewed by:
Alexander Kholodov,
University of Alaska Fairbanks, United States
Oksana Zanina,
Institute of Physical-Chemical and Biological Problems in Soil Science (RAS), Russia

****Correspondence:***
I. D. Streletskaya
irinastrelets@gmail.com

Specialty section:
This article was submitted to Cryospheric Sciences, a section of the journal Frontiers in Earth Science

Received: *10 June 2021*
Accepted: *11 October 2021*
Published: *19 November 2021*

Citation:
Streletskaya ID, Pismeniuk AA, Vasiliev AA, Gusev EA, Oblogov GE and Zadorozhnaya NA (2021) The Ice-Rich Permafrost Sequences as a Paleoenvironmental Archive for the Kara Sea Region (Western Arctic). Front. Earth Sci. 9:723382. doi: 10.3389/feart.2021.723382

INTRODUCTION

The ice-rich Quaternary deposits including ground ice of various types are widely present at the Western Siberia coast and the Kara Sea shelf. Despite that permafrost studies in Western Siberia were conducted for more than a hundred years, the conditions of the Quaternary sediments and ground ice genesis are still under debate.

Over the last 200 thousand years of Quaternary history, marine sedimentation has repeatedly changed with continental sedimentation on the coastal plains of the Western Arctic (Molodkov and Bolikhovskaya, 2009). Many geological sections of marine Pleistocene deposits include massive

tabular ground ice (MTGI). The origin of these extensive ice bodies in Western Siberia is under continued debate. Some studies argued that it is buried glacial ice of Late Pleistocene (Solomatin, 1982; Kaplyanskaya and Tarnogradsky, 1986; Gataullin, 1988; Forman et al., 2002; Astakhov, 2009). The authors of this work support non-glacial genesis of the ice (Streletskaya and Leibman, 2003) and explain the position of the MTGI at the interface between two lithologic units: sandy sediments beneath and clay sediments above the ice body. Water segregation and intrusion through the deposits leave evidence of both water sources and the aquifer properties in the resulting MTGI. The following line of evidence support this explanation: i) MTGI bodies are found in littoral clay sediments of the Late Pleistocene (Streletskaya et al., 2008; Streletskaya et al., 2009); ii) heavy stable isotope composition and relationship between oxygen and hydrogen isotopes show that the MTGI in the marine sediments were formed *in-situ* within the ground (Streletskaya et al., 2012a; Streletskaya et al., 2013); iii) chemical signatures of the sediments and the MTGI indicate the possibility of intrusive origin of the MTGI (Streletskaya and Leibman, 2003; Streletskaya et al., 2006; Oblogov, 2016); iiii) high concentrations of methane trapped in the air bubbles within the MTGI and the stable isotope analysis of methane are indicative of ground ice formation (Streletskaya et al., 2018; Dvornikov et al., 2019; Oblogov et al., 2020; Semenov et al., 2020).

Upper 10–15 m of the Late Pleistocene - Holocene sections typically consist of ice-rich continental sediments of polygenetic origin containing syngenetic Ice Wedges (IW) of two ages (Late Pleistocene and Holocene). The formation of syngenetic IW occurs as a result of the snow and meltwater refreezing in the frost cracks (Mackay, 1974). In Nothwest Siberia and Yenisei North frost cracks form primarily between mid-January and mid-March (Podborny, 1978). Meltwater entering the cracks freezes rather rapidly preventing isotopic fractionation (Michel, 1990). The stable oxygen isotopic composition of ice wedges is correlated with mean winter and January temperatures (Vasil'chuk, 1992; Nikolaev and Mikhalev, 1995; Vasil'chuk, 2006; Streletskaya et al., 2015). In the Kara region many authors have described syngenetic polygonal-wedge ice occurring in the Pleistocene-Holocene mainly silty sediments (Danilov, 1978; Karpov, 1986; Kanevskiy et al., 2005; Vasil'chuk, 2006; Kritsuk, 2010). The most extensive complexes of ice-rich deposits containing syngenetic IW are found in the northern East Siberian lowlands, where they are called Ice Complex formations. The issue of terminology, genesis and distribution of ice complex (or "yedoma") causes a lot of discussion (Popov, 1953; Tomirdiaro, 1980; Péwé and Journaux, 1983; Schirrmeister et al., 2003; Bolshiyanov et al., 2008). Currently, the point of view about the polygenetic origin of this unique phenomenon is becoming more and more popular (Bolikhovsky, 1987; Romanovskiy, 1993; Kanevskiy et al., 2011). By the sediments of the ice complex, we mean ice-rich mainly silty, silty-sandy sediments with inclusions of organic remains, containing syngenetic IW. In contrast to Yakutia, the ice complex of West-Siberian North has a smaller thickness (up to 12 m), includes smaller IW and formed in the last stage of the Pleistocene and Holocene.

Ongoing debate about the origin of ice and insufficiently detailed studied of ice-rich permafrost sequences require further attention. This review summarizes the data on the ice-rich sediments of the Western Siberia coast obtained during numerous expeditions. The main goal of this study is therefore to identify the major characteristics of the ground ice and Quaternary deposits of Western Siberia, and to characterize permafrost evolution from the Late Pleistocene to the present. The specific objectives are to: i) collect all available data of the permafrost sections of Western Yamal, Gydan, and Yenisei North; ii) describe the cryostratigraphy of frozen sediments; iii) establish the conditions for the formation of ice-rich sediments and ground ice; iiii) develop a conceptual model of the Western Arctic paleogeography and show the difference with the ice complex formation in the East Siberia. This work summarized materials collected by authors during expeditions to the Kara Sea region over the last 16 years. **Table 1** presents location of key sites (**Figure 1**), time of fieldworks and main publications for each study site previously conducted by authors.

METHODS

Fieldwork

Eight Quaternary sections of the Western Siberia coast were documented, photographed and sketched, indicating the height of all layers and sampling locations. The sediments were collected at 0.3–1.0 m intervals for grain-size, organic matter and biostratigraphic indicators. Peat, wood fragments, and animal bones were collected for dating. The ground ice was sampled across the bedding of the ice body (the IW and MTGI is sampled along the horizontal and vertical profiles). When possible, the samples were transported to the laboratory in a frozen state. In the field, preliminary preparation and preservation of samples for transportation to the laboratory was carried out. Some of the samples in the form of monoliths of frozen sediments and ice were transported to laboratories in mobile refrigerators.

The gravimetric ice content (wt%) was estimated immediately after thawing by relating the weight of the frozen sample to the weight of the dry sample, expressed as weight percentage (%). More than 1,000 sediment samples were collected.

Stable Water Isotopes ($\delta^{18}O$, δD)

Stable isotopes $\delta^{18}O$ and δD from 344 samples were determined using Finnigan MAT Delta-S mass spectrometer at the isotope laboratory of the Institute for Polar and Marine Research (Potsdam, Germany). Isotopic composition is expressed in ppm (‰) relative to the V-SMOW standard (**Supplementary Table S2**). The analytical precision is better than ±0.8‰ for δD and ±0.1‰ for $\delta^{18}O$ (Meyer et al., 2000). The isotopic values of individual parameters are plotted in the δD – $\delta^{18}O$ diagram and compared to the Global Meteoric Water Line (GMWL) to determine the genesis of ground ice. The deviation of points from the GMWL is estimated by the amount of excess deuterium (d_{exc}).

TABLE 1 | Location of studied ice-rich permafrost sites and corresponding site-specific publications.

Location	Coordinates		Years of field studies	Main publications
	N	E		
MS – Marre-Sale Polar Station	69°41	66°48	2004–2019	Kanevskiy et al. (2005), Streletskaya et al. (2006), Streletskaya et al. (2013), Streletskaya et al. (2018); Oblogov et al. (2020)
EM - Ery-Maretayakha River Mouth	71°50	75°13	2010	Oblogov et al. (2012), Streletskaya et al. (2012a), Streletskaya et al. (2013)
MA-Matyuisale trading post	72°00	76°25	2010	Pismeniuk et al. (2019)
PS - Paha-Sale Cape	71°17	77°34	2010	Oblogov et al. (2012), Streletskaya et al. (2012b), Streletskaya et al. (2013)
SB - Sibiryakov Island	72°43	79°06	2008–2009	Gusev et al. (2011), Gusev et al. (2013), Streletskaya et al. (2012a), Oblogov, (2016)
DI – Dikson Settlement	73°30	80°33	2008–2010	Streletskaya et al. (2007), Streletskaya et al. (2011), Streletskaya et al. (2013), Oblogov, (2016)
KR – Khrestyanka River Mouth	72°58	80°51	2007	Streletskaya et al. (2007), Streletskaya et al. (2013), Oblogov, 2016
SK - Sopochnaya Karga Cape	71°53	82°40	2007–2010, 2014	Streletskaya et al. (2007), Streletskaya et al. (2011), Streletskaya et al. (2013), Oblogov, (2016)

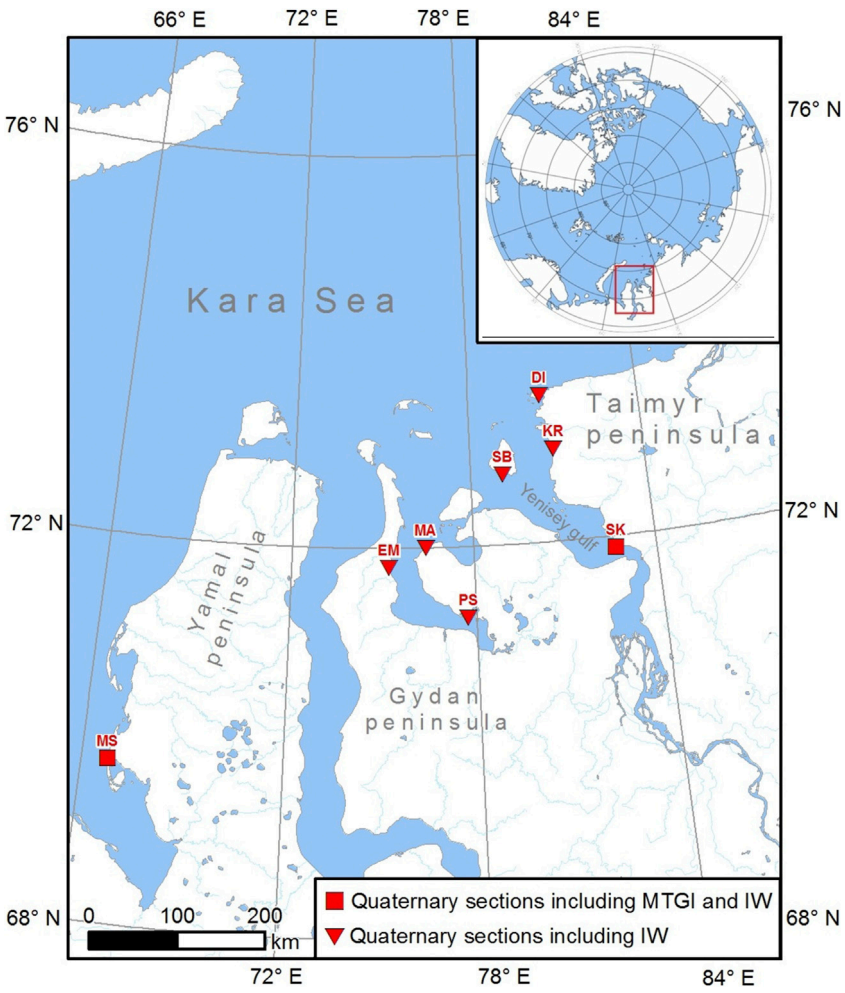

FIGURE 1 | Study region and location of key sites indicated in **Table 1**.

OSL and Radiocarbon Dating

Quaternary sediments were dated using radiocarbon dating (^{14}C), small samples was dated using accelerating mass spectrometry (AMS), and optical infrared stimulated luminescence (IR-OSL). The shells of marine and freshwater mollusks were dated by ^{14}C methods and AMS; wood remains, peat and mammalian bone remains by ^{14}C; enclosing parental strata such as sands and silts by IR-OSL.

Radiometric dating of 41 samples was held in in Geomorphology and Palaeogeography Laboratory of Polar Regions and the World Ocean (KÖPPENLab, Institute of Earth Sciences, St. Petersburg State University). Radiocarbon dating using the AMS was determined at the AMS Laboratory at the University of Arizona (two samples). Direct dates were calibrated using the «OxCal 4.4» program (https://c14.arch.ox.ac.uk). All radiocarbon dates through this paper are reported as uncalibrated ages (**Supplementary Table S1**).

OSL dates has been obtained from nine samples in IR-OSL in the Laboratory of Geochronology of the Quaternary Period, Institute of Geology, Tallinn University of Technology (IG TTU) (**Supplementary Table S1**).

Lithology and Geochemistry

The complex of lithological and geochemical analyses of soil and ground ice were conducted in the Laboratory of Lithology and Geochemistry of All-Russian Research Institute for Geology and Mineral Resources of the World Ocean (VNIIOceangeologia) in St. Petersburg, Russia. Grain size was determined by sieving and pipette analysis. The ion composition of the Quaternary deposits was determined from the water extract. Ground ice melts were preliminarily filtered to remove suspended matter. Subsequently, both in the water extract and in the ice filtrates, the concentrations of K, Na, Sr were determined by flame photometry, and Ca, Mg, Cl, SO_4, HCO_3 were determined by titration. Mineralization of ice was calculated from the sum of the cations and anions concentrations. Total organic carbon (TOC) was determined on Shimadzu TOC-VCSH analyzer using an IR detector with preliminary catalytic oxidation.

Methane concentrations were also determined in the two key study sites in the ground ice (Marre-Sale and Sopochnaya Karga Cape) and in enclosing ice sediments (Marre-Sale). Out of 920 samples collected at the Marre-Sale, 214 were collected from ground ice, 393 from frozen sediments. 25 samples were collected from ground ice at Sopochnaya Karga Cape. During 2012–2013 field seasons, the degassing of ice monolith samples was performed using a dynamic method of degassing by SUOK-DG degassing unit (Patent (19) RU (11) 2348931 (13) C1). Gas composition was determined by chromatography with flame ionization detector (FID) Shimadzu GC-2014 (Japan). After 2013, samples were degassed using a «head space» method (Alperin and Reeburgh, 1985) in the field and sent to the laboratory. Concentration of methane in gas phase was also determined in the Institute of Physical, Chemical, and Biological Problems in Soil Science RAS (Pushchino, Russia) using a gas chromatograph HPM.4 (Russia) with flame ionization detector. The difference of results obtained by two methods did not exceed the measurement accuracy. To determine the genesis of the MTGI, six samples collected at Marre-Sale were analyzed for δD (CH_4) content in the ISOLAB B.V. laboratory, Netherlands. Summary characteristics of the ground ice chemical composition provided in the **Supplementary Table S2**.

RESULTS

Marre-Sale Polar Station (MS)

The westernmost key site is located on the Yamal Peninsula near the Marre-Sale polar station. The Quaternary section here is well-studied and remains a reference for permafrost research (Forman et al., 2002; Kanevskiy et al., 2005; Streletskaya et al., 2006; Streletskaya et al., 2009; Kritsuk, 2010; Slagoda et al., 2012).

Two complexes of Quaternary deposits were investigated in the coastal cliff exposure about 30 m high (**Figure 2**). The upper complex on average 10 m thick consists of the Late Pleistocene-Holocene continental (alluvial, lacustrine) non-saline sands and sandy loams. Holocene sands, sandy loams and fragmentary peat found from the surface to 2–4 m depth (Unit 1). These deposits formed from 8.2 to 1.2 ka BP (**Supplementary Table S1**) (Forman et al., 2002; Slagoda et al., 2012). Sodium ions and bicarbonate ions predominate in the composition of water-soluble salts. The TOC content varies from 0.1 to 0.4%.

Holocene deposits are overlaying the Late Pleistocene deposits represented by sandy loams with layers of silt with inclusions of dark organic matter, lenses and pieces of peat and plant roots (2.0–10.0 m; Unit 2). The lower boundary of the complex contains an interlayer (0.2–0.3 m) of coarse-grained sands with fragments of wood, dark-colored pebbles and lenses of pure ice (2–5 cm). The salinity of sediments does not exceed 0.05%, sodium and bicarbonate ions dominate the composition of water-soluble salts. The values of TOC vary from 0.4 to 0.6%. The deposits have belt-like cryogenic structure. Interlayers are characterized by low ice content and a massive cryogenic structure (the Wt% is 16–20%), highly icy interlayers have small vertically oriented ice lenses (the Wt% is 35–55%). The average methane concentrations in the upper complex of Quaternary deposits are between 147 ppmV (0.08 ml/kg) and 269 ppmV (0.11 ml/kg) (Streletskaya et al., 2018).

The upper complex of continental deposits contains syngenetic IW of different ages. Larger wedges, 2.0–2.5 m wide at the top and 6–7 m long, form a grid with a polygon side of 10–20 m. The ends of the wedges penetrate the MTGI. According to S. Forman (2002), active formation of syngenetic IW occurred in MIS 3. The content of stable isotopes in the Upper Pleistocene ice wedges varies from −27.0‰ to −16.6‰ for oxygen, and from −208.0‰ to −123.7‰ for deuterium. The deuterium excess is 7.8‰ (**Supplementary Table S2**). Smaller Holocene wedges, 0.5–1.0 m wide at the top and 1.5–2.0 m long, form a grid with a polygon side of 6–8 m. The dating of peat fragments from IW gave an age close to 8 ka BP (**Supplementary Table S1**) (Forman et al., 2002). The stable isotope composition in Holocene ice wedges for oxygen varies in the range from −22,8‰ to −11.1‰ and for deuterium from −170.8‰ to −89.9‰ (**Supplementary Table S2**). The deuterium excess is 8.2‰. Mineralization of IW are about 84 mg/L for Holocene and 70 mg/L for Late Pleistocene IW respectively (**Supplementary Table S2**). Methane concentrations are 40 ppmV (0.04 ml/kg) in Pleistocene IW and 146 ppmV (0.16 ml/kg) in Holocene IW respectively (Streletskaya et al., 2018).

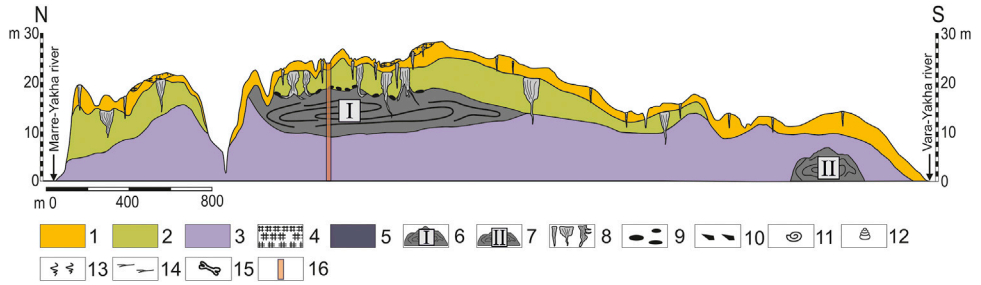

FIGURE 2 | Generalized cross-section of the exposure at Marre–Sale polar station (redrawn after to Forman et al. (2002), Kanevskiy et al. (2005), Streletskaya et al. (2006), Streletskaya et al. (2009), Kritsuk (2010)). Legend: 1 — Unit 1 – alluvial, eolian, deluvial solifluction (or slope), lacustrine deposits (MIS 1); 2 — Unit 2 – undifferentiated alluvial, alluvial-marine, lacustrine, slope deposits (MIS 2–3); 3 — Unit 3 – undifferentiated marine, lagoon-marine deposits (MIS 6–4); 4 — peat (without distinction as to age); 5 — bedrocks; 6 — MTGI (1 type); 7 — MTGI (2 type); 8 — ice wedges shown outside of scale (without distinction as to age); 9 — rounded pebble; 10 — coarse gravel; 11 — sea mollusks; 12 — fresh-water lacustrine shells; 13 — detritus inclusions; 14 — wood debris inclusions; 15 — the place of mammoth carcass find; 16 — sections of grain size sampling in accordance with the **Figure 10**.

The lower complex represented by the saline marine clays and loams, which formed prior to MIS 3 (Unit 3). The salinity of clays varies from 0.02 to 0.30% with sodium chloride composition. The layer has no visible organic inclusions; the mean TOC is 0.84%. The clays have a large-scale reticulate cryostructure (Wt% is 30–60%). Marine clays were freezing epigenetically after of retreating sea. Average concentration of methane in clay (or loam) is 3,875 ppmV (2.02 ml/kg) (Streletskaya et al., 2018).

Two types of MTGI are included in the lower complex of marine sediments. The MTGI of first type located in the contact of the saline marine clays and continental sandy-clayey sediments. MTGI is 3–10 m thick and 300 m long. Sandy loam and sand alternating with dislocated ice layers up to 1.5 m thick represent it. The particle size distribution of mineral inclusions in ice varies: sandy inclusions are from 10 to 91%, silty - from 6 to 62%, clay - from 10 to 36%. In general, the amount of sand particles in the MTGI decreases with depth, while the proportion of clay and silt increases. Heavy minerals of the sand fraction in clay are well sorted. The cryostructure of the ice-soil interlayers in the MTGI is microlenticular. Folded deformations are often observed within MTGI. The layer contains inclusions of well-decomposed organic matter. The TOC content in MTGI increases to 1.1–1.3%, in presence of silty and clay particle inclusion within the ice, but only 0.16%, where sandy particles dominate. Salinity of clay layer in MTGI reaches 0.7%. The composition of the salts remains sodium chloride. The content of stable isotopes in the MTGI varies from −21.5‰ to −17.2‰ for oxygen, and from −165‰ to −129‰ for deuterium (**Supplementary Table S2**). The deuterium excess is 7.9‰. The second type is the clear homogeneous MTGI in marine clay with 6–8 m thick and 150–200 m long, visible part submerging below the sea level. The transition from overlying clay sediments to MTGI is marked by the change in cryostructure from layered to reticulate and coarse-block (block size about 30 × 20 cm, ice lenses 0.5–1 cm thick). The MTGI have rare mineral inclusions. Based on the results of mineralogical analysis clay particles predominate, the presence of marcasite indicates hydrogen sulfide contamination of freezing water. The isotope composition (**Supplementary Table S2**) of ice varies from −21.9 to −7.5‰ for oxygen and from −163.7 to −67.9‰ for deuterium (D), d_{excess} is 6.4‰. MTGI has unevenly distributed rounded and horizontally elongated air bubbles of 1–2 mm in diameter. The air bubbles contain methane. Methane concentrations from bubbles into MTGI are on average 1,413 ppmV (1.57 ml/kg) for the first type and 558 ppmV (0.62 ml/kg) for the second type respectively (Streletskaya et al., 2018). Mineralization of MTGI varies from 23 to 260 mg/L for the first type and from 32 to 218 mg/L for the second type of ice respectively (**Supplementary Table S2**).

Ery-Maretayakha River Mouth (EM)

The cross-section (**Figure 3**) of the western coast of the Gydan Bay is exposed in the coastal cliff consisting of thermo-denudation surfaces (15–28 m a.s.l) and the thermo-abrasive cliff descending to the modern beach near the Ery Maretayakha River mouth (Oblogov et al., 2012; Streletskaya et al., 2013). Two layers of IW are exposed in the section. Vasil'chuk (1992) obtained dates of the Late Pleistocene peat-mineral complex at Mongatalyangyakha river mouth, close to the section from 34.8 (3.5 m a.s.l.) to 26.3 (5.9 m a.s.l.) ka BP (**Supplementary Table S1**). As a result, the age of the lower part of the Ery-Maretayakha section relates to MIS 3 (Kargino horizon in the modern Pleistocene stratigraphic scheme of West Siberia).

The upper part of the EM section to a depth of 4.7 m consists of ice-rich frozen lacustrine deposits. Partially decomposed peat alternate with large interlayers of pure ice near the surface. The age of the peat is 9.5 ka BP (**Supplementary Table S1**) (Oblogov et al., 2012). Lower, ice-rich sandy silts (Unit 1) contain peat, plant roots and fossils of fresh-water mollusks (the silt particles content is more than 54%). The value of TOC reaches 0.9%. The peat deposits are dated to the Early Holocene (**Supplementary Table S1**). The cryogenic structure is belt-like; the Wt% is on average 53%. Holocene IW are 1.2 m wide at the top and 3.6 m long. Late Pleistocene IW are 2.5 m wide at the top and more than 10 m long. The isotopic composition of the upper-layer IW

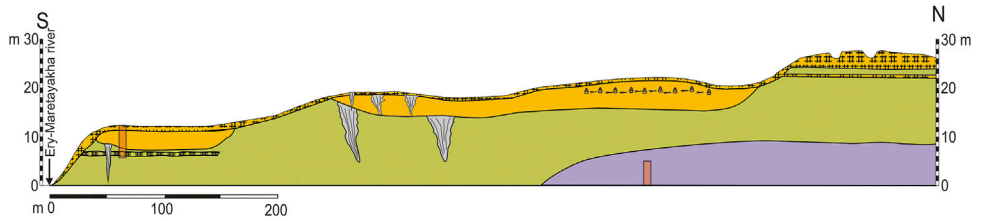

FIGURE 3 | Generalized cross-section of the exposure at Ery-Maretayakha River mouth (adopted from Oblogov et al. (2012)). See legend for **Figure 2**.

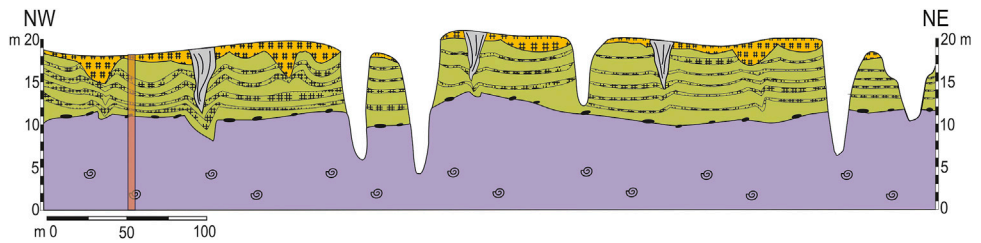

FIGURE 4 | Generalized cross-section of the exposure at Matyuisale trading post (redrawn after to Pismeniuk et al. (2019)). See legend for **Figure 2**.

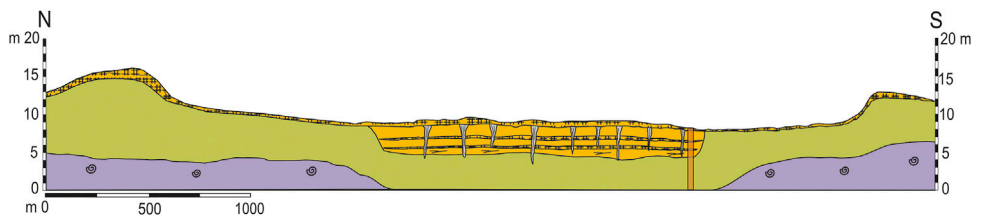

FIGURE 5 | Generalized cross-section of the exposure at Pakha-Sale Cape (redrawn after to Oblogov et al. (2012)). See legend for **Figure 2**.

changes from −23.6 to −18.3‰ for oxygen and from −179.9 to −134.3‰ for deuterium; the deuterium excess changes from 9 to 12‰ (**Supplementary Table S2**). Mineralization of Holocene ice is 212 mg/L (**Supplementary Table S2**).

Unit 2 represents Late Pleistocene alluvial silty sandy loams. The sandy fraction in the unit increases with depth, in contrast TOC decreases to 0.2%. Closer to the river mouth silty and sandy loams alternate with fine-grained sands and peat with massive cryostructure. The Wt% decreases with depth from 54 to 27%. The peat interlayer in sandy sediments has the age of 26.3 ka BP (**Supplementary Table S1**). The content of oxygen and hydrogen stable isotopes in the Late Pleistocene ice wedge does not change with depth and is from −24.6 to −22.6‰ for oxygen and from −193.1 to −176.5‰ for deuterium; the deuterium excess does not exceed 6–7‰. Mineralization of Late Pleistocene ice is 126 mg/L (**Supplementary Table S2**).

In the northern part of the section, the sandy silts from the 20 m depth cover ice-rich clays (Unit 3). The clays have a high content of TOC (0.89%) and the Wt% from 26 to 33%. The clays have reticulate cryogenic structure, which indicates the epigenetic freezing of deposits.

Matyuisale Trading Post (MA)

The cross-section near the Matyuisale trading post consists of two units (**Figure 4**). The upper is peat-mineral complex with the inclusion of ice wedges; the lower one is represented by saline marine clays. The peat layers dated from 41.2 ka BP at 7 m a.s.l. to 8.7 ka BP at 9.1 m a.s.l. (**Supplementary Table S1**). Accordingly, continental conditions were established in the region of 41–42 thousand years ago.

The thickness of the peat-mineral complex (Unit 2) varies along the section from 5 to 10 m. It represents alternating layers of peat, yellow-brown sands, sandy loams and loams with belt-like cryogenic structure. The deposits are silty with silt particles comprising up to 85%. There is a lot of visible organic matter in the sediments; the organic carbon content varies from 0.49% in silty clays to 2.15% in sandy loams. The Wt% of the sediments in the upper part varies from 39.8 to 71.8%. At the boundary with the underlying saline clays, brown-gray silty sandy loam with

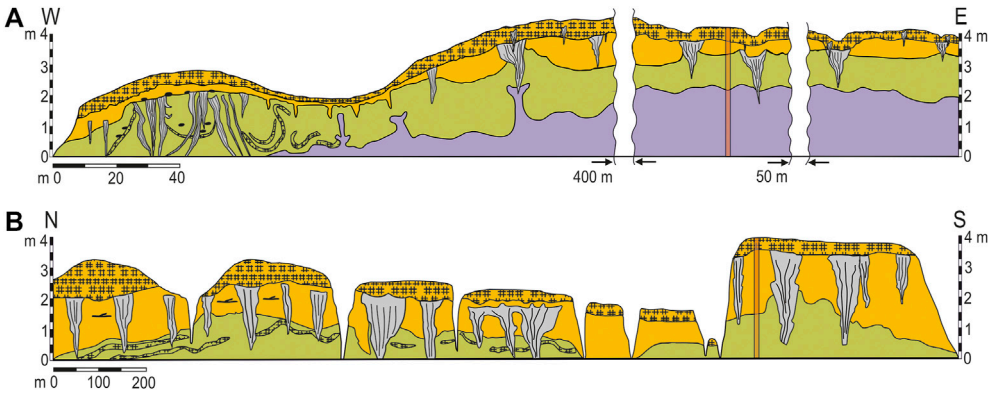

FIGURE 6 | Generalized Quaternary section of the exposure at Sibiryakov island (**A** – southern coast; **B** – western coast) (redrawn after to Streletskaya et al. (2012b), Oblogov (2016)). See legend for **Figure 2**.

interlayers of fine-grained sand and a distinct 0.1 m pebble horizon is present. The TOC in the layer is about 0.41%. The Wt% sediments at the lithological boundary with clays is 36.1%.

In the upper part of the peat-mineral complex, ice wedges are 1.5–2.0 m wide at the top and more than 5 m long. Stable isotope content in ice varies from −19.2 to −17.2‰ for oxygen and from −143.5 to −127.9‰ for deuterium (**Supplementary Table S2**). The deuterium excess is on average 9‰. The ice mineralization is 37 mg/L (**Supplementary Table S2**). At the lateral contacts of some wedges with the enclosing sediments, a distinct iron framing, repeating the shape of the wedge is observed. This indicates that its formation occurred along the ice-wedge casts of an older ice wedge. Late Pleistocene IW completely thawed in the area. The Holocene ice wedges occasionally infiltrated into ice-wedge casts.

In the lower part of the section (up to 15 m a.s.l.) dark gray saline clays are exposed (Unit 3). Cryogenic structure differs across the section from reticular to prismatic. There is no visible organic matter in the clays, but the values of TOC are quite high (0.48–0.53%). The clays have a high content of sedimentary marine (NaCl) salts, which indicates their marine genesis. Salinity is more than 0.37%. The marine unit contains very rare fragments of mollusks (Hiatella arctica, Macoma calcarea, etc.). The Wt% varies from 36.1% (11 m a.s.l.) in sandy loams to 16.4% (6 m a.s.l.) at the boundary with clays.

Pakha-Sale Cape (PS)

In the 10–17 m high coastal cliff from Paha-Sale Cape to Nyada-Sale Cape, Late Pleistocene-Holocene continental sediments cover older marine unit (**Figure 5**).

The lens of lacustrine sediments (Unit 1) up to 4–6 m thick and 1,200 m long contains organic-rich sandy loams (the TOC reaches 1%) with a layered cryostructure. Light sandy loams at 2–4 m depth transform into heavy sandy loam. The silt particles content increases from 35% at 1.4 m depth to 56% at 3.7 m depth. The Wt% increases from 33% at 1.4 m depth to 64.7% at 3.2 m depth. The cryostructure of the sandy loam is finely reticulate, postcryogenic. These are deposits characteristic of the talik. The lake was filled with sediments from the Early to Middle Holocene (from 8.8 to 6 ka BP; **Supplementary Table S2**). Lacustrine deposits include IW complex. Ice-wedges have the 0.2–0.5 m wide at the top and the 2–5 m long. The IW isotopic values are on average −19.1‰ for oxygen and −146.2‰ for deuterium; the deuterium excess is 7.2‰. Mineralization of ice is 17 mg/L (**Supplementary Table S2**). Gray fine-grained sands of Unit 2 underlie silty sandy loam. The sands have the massive cryostructure. The Wt% is 22.4%. Marine clays with a rich fauna of marine mollusks (Unit 3) underlie the section. The Wt% at the contact of clays and silty sandy loam is 64.1%.

Sibiryakov Island (SB)

Sibiryakov Island located at the northern part of the Yenisei Gulf. It is relatively flat with average height decreases from the central part (25–33 m a.s.l.) to the coastal area (3–5 m a.s.l.).

Southern coastal cliff about 2.0–4.5 m a.s.l. consists of three units (**Figure 6A**). Holocene peat with an admixture of sand up to 0.5–1.5 m thick form the uppermost layer. Peat began to form at the surface around 3.7 ka BP (**Supplementary Table S1**). Under the peat layer, a layer of gray oblique-bedded sandy loams and sands (Unit 1) is located and has plant remains. The cryostructure is massive or lenticular. The upper and lower boundaries are gradual. The Unit 2 is composed of stratified iron rich sands up to1.2–2.0 m thick with traces of deformation, inclusions of pebbles, gravel, plants and peat. The content of water-soluble salts in sands does not exceed 0.06%. The average value of TOC in the sands is 0.26%. The deposits have massive cryogenic structure. The Wt% is 21–30%. Content of silt fraction in deposits reaches 75%. The amount of TOC increases to 1.3%. The unit dated from 13.3 to 31.4 ka BP (**Supplementary Table S1**). Sands overlie dark gray saline (salinity is 0.7%) silty sandy loam of marine genesis (Unit 3). The deposits formed in MIS 3, the older date is 45.8 ka BP obtained by the IR-OSL method (**Supplementary Table S1**).

The western coastal cliff up to 3.5 m a.s.l. (**Figure 6B**) consists of two units. Autochthonous peat is exposed from the surface to a depth of 0.5–1.5 m. Below the section, peat is replaced by layered

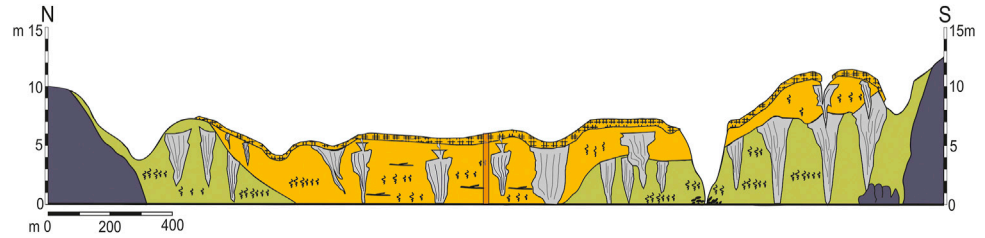

FIGURE 7 | Generalized cross-section of the exposure at Dikson village (redrawn after to Streletskaya et al. (2013)). See legend for **Figure 2**.

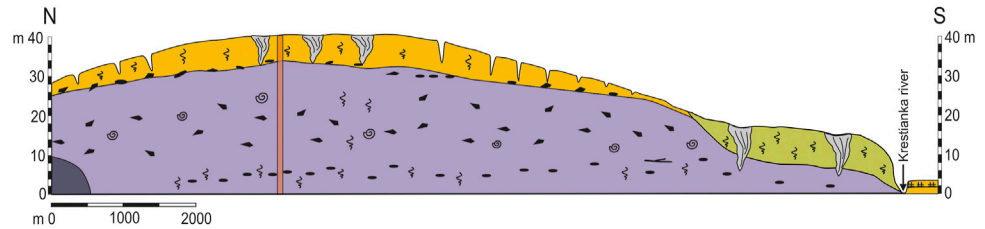

FIGURE 8 | Generalized cross-section of the exposure at Khrestianka River mouth (redrawn after to Streletskaya et al. (2013)). See legend for **Figure 2**.

gray silty sandy loam (0.5–3.0 m thick) with traces of iron, lenses of sand, inclusions of peat and wood. The date from sandy loams, obtained by the IR-OSL method, is 8.6 ka BP (Gusev et al., 2013). Ice wedge casts are present. The postcryogenic texture indicates syngenetic formation and freezing of the sediments. Sandy loams have massive cryogenic structure (Wt% less than 25%), sandy loams are ice-rich (Wt% is 90%) with a lenticular-mesh cryostructure only at contacts with ice wedges. From a 2.5 m depth sandy loams are ice rich with lenticular and suspended cryostructure (the Wt% is more than 60%). The sands underlying the sandy loam have a massive cryostructure (the Wt% is 30%).

In the sandy loams, ice wedges up to 2 m height spaced by 8–10 m were found. The width of the IW at the top does not exceed 1.5 m. The sandy loam enclosing ice wedges are strongly iron-rich, some of the IW repeat the form of ice wedge casts, penetrate into the sediments of Unit 2 and possibly sediments of Unit 3. The isotope content in ice wedges varies from −22.1 to −16‰ for oxygen and from −167.5 to −121‰ for deuterium. Mineralization of ice is about 58 mg/L (**Supplementary Table S2**).

Dikson (DI)

The most complete section of Quaternary sediments was studied in the Dikson area where two layers of IW are exposed in the coastal cliff (**Figure 7**).

The Quaternary section consists of two units containing syngenetic IW. According to the results of radiocarbon dating (**Supplementary Table S1**), the Holocene unit accumulated 9.8 to 3.7 ka BP (Gusev et al., 2011). The deposits are homogeneous in particle size distribution and consist of silty-sized particles, which number increases with depth from 82 to 96%. The TOC in the sediments of upper unit 1 is 0.6–1.2% and reaches 2.1% due to inclusions of peat and wood fragments. In the deposits including Late Pleistocene IW (Unit 2), the TOC is about 0.6%. Organic matter is uniform in the section. The ice-rich deposits (Wt% is over 86%) have a rhythmically layered structure typical for syngenetic deposits.

The visible thickness of the deposits is about 10 m, but the IW continues below the sea level. The width of the Late Pleistocene wedges at the top reaches 6 m, the thickness - 10 m and more. The width of the wedges of the Holocene unit at the top is up to 4 m, the thickness varies from 2–3 to 7 m. Late Pleistocene IW in the area have a width from 0.4 to 3 m at top and more than 5 m thickness. The isotopic composition of Pleistocene IW show changes of values from -26.8 to -22,9‰ for oxygen and from -205 to -175‰ for deuterium. The isotopic values of the Holocene IW varies from -21.2‰ to -14.8‰ for oxygen and from -159‰ to -108‰ for deuterium (**Supplementary Table S2**) (Streletskaya et al., 2011). Ice mineralization increases from 47 mg/L (Holocene IW) to 360.5 mg/L (Late Pleistocene IW) (**Supplementary Table S2**).

Khrestianka River Mouth (KR)

Quaternary deposits are overlaying Permian bedrocks in the 12–40 m high coastal cliff of the Yenisei Bay from Cape Makarevich to the Khrestianka River mouth (**Figure 8**).

Holocene deposits (Unit 1) are exposed in the southern part of the section. The main section part is a levelled surface of the Yenisei terrace 35–40 m high with baydzherakhs (residual-thermokarst mounds). To the south, the surface of the terrace descends to 18–23 m high and turns into the slope of the Krestyanka River valley (12–20 m a.s.l.). The upper part of the

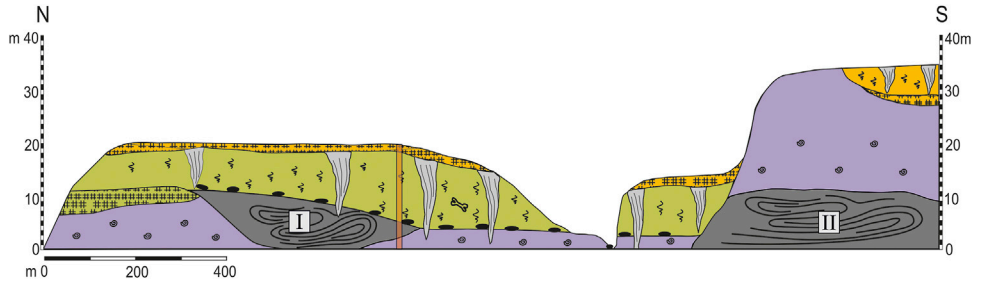

FIGURE 9 | Generalized cross-section of the exposure at Sopochnaya Karga Cape (redrawn after to Streletskaya at al. (2013)). See legend for **Figure 2**.

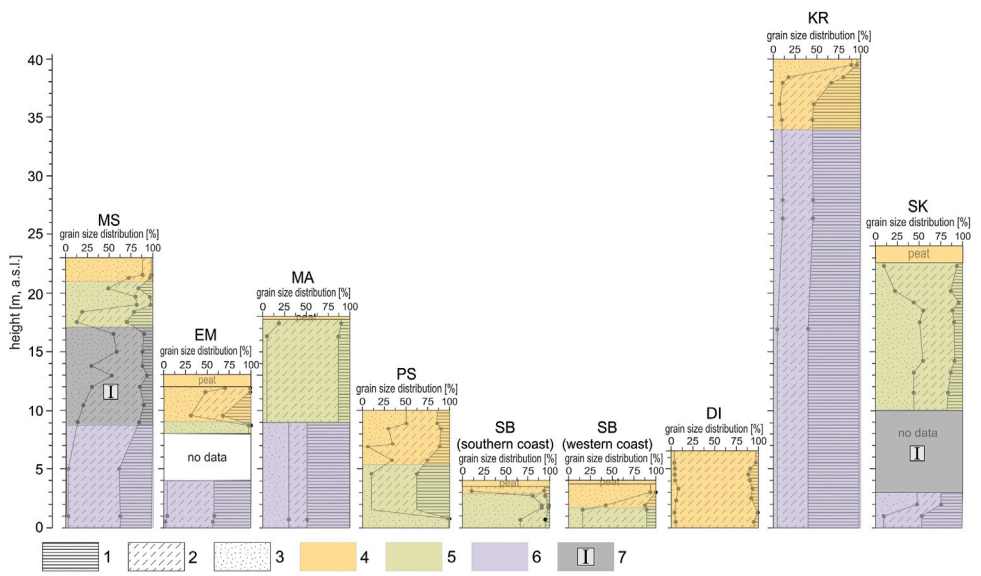

FIGURE 10 | Grain size distribution patterns of studied ice-rich permafrost sequences. Legend: 1–3 – Grain size composition in accordance with the V.V.Okhotin (1933) classification: 1 – clay, loam; 2 – sandy loam; 3 – sand; 4–6 – Units: 4 – Unit 1 – alluvial, eolian, deluvial solifluction (or slope), lacustrine deposits (MIS 1); 5 – Unit 2 – undifferentiated alluvial, alluvial-marine, lacustrine, slope deposits (MIS 2–3); 6 – Unit 3 – undifferentiated marine, lagoon-marine deposits (MIS 6–4); 7 – MTGI (1 type).

section contains dark brown silty sandy loams (Unit 2) with peat fragments 5–7 m thick. Silt fraction in deposits reaches 83%. Sandy loams contain 0.05–0.14% of soluble salts with prevailing sodium and chloride ion composition. Sandy loams have numerous detritus; the TOC content is 0.7–0.9%. The deposits are ice rich (the Wt% reaches 80%), have belt-like cryostructure and contain large syngenetic IW. Ice wedges are about 9 m thick and 3–4 m wide at the top and form the polygonal topography. The average values of the isotope composition vary from −23.5 to −22.0‰ for oxygen and from −179.7 to −167.7‰ for deuterium. Within a single wedge, isotopic composition is rather similar (Streletskaya et al., 2011). Deuterium excess is from 8.2 to 10.2‰) (**Supplementary Table S2**). The lower part is represented by marine clays of Pre-Kargino age (Unit 3). The age and genesis of this unit were previously discussed (Streletskaya et al., 2013; Gusev et al., 2016; Oblogov, 2016).

Sopochnaya Karga Cape (SK)

Several exposures of Quaternary deposits containing MTGI and ice wedges (**Figure 9**) were studied 6 km from Sopochnaya Karga Cape (Streletskaya et al., 2011; Streletskaya et al., 2013).

The upper part of the section from the surface to 1–2 m depth is represented by poorly decomposed peat. The formation of this layer began about 11 ka BP (Gusev et al., 2011). In the southern part of the section at 30–35 m a.s.l., Holocene lacustrine deposits (Unit 1) with IW 5 m thick and 0.4 to 3.0 m wide are exposed. These deposits are ice-rich (the Wt% exceeds 80%) and have distinctive belt-like cryogenic structure. The underlying peat layer is dated to the Holocene optimum (**Supplementary Table S1**) (Streletskaya et al., 2012b). The range of $\delta^{18}O$ in Holocene IW is −23.3‰ to −17.1‰, and the range of δD is −175‰ to −122‰. The deuterium excess is 11.6‰ (Streletskaya et al., 2011). Ice mineralization from Holocene IW is 22 mg/L (Supplementary

Table 2). Methane concentrations in Holocene ice wedges on average are 74 ppmV (0.08 ml/kg) (Streletskaya et al., 2018).

Stratified yellow-gray silty sandy loams and sands with interlayers of peat 4–10 m thick are located below (Unit 2). These deposits contain plant roots; the TOC reaches 2.0%. Salinity does not exceed 0.06%. Bicarbonate and sodium ions prevail among the ions. The amount of silt particles and organic impurities decrease with depth, sandy loam turns into coarse-grained and gravelly sands. Grain-size and mineral analysis of the gravel horizon present at the contact of clays and sands suggests alluvial channel of a large river downstream. The carcass of a woolly mammoth was found at a depth of 6 m in 2012. The dates of it ranged from 42.2 ka BP to 47.3 ka BP (Maschenko et al., 2017; **Supplementary Table S1**). In the north of the section central part, under the sandy loam stratum, peat interlayers are exposed, the age is more than 42.3 ka BP (Streletskaya et al., 2013). Sandy loam and sands (MIS 3- MIS 2) contain syngenetic IW about 10 m thick and 2–3 m wide at the top. The lower narrow parts of the wedges penetrate into the clays by 0.5–1.0 m, in some parts of the section they continue below sea level. The values of isotopic composition range from −26.9 to −21.7‰ for $\delta^{18}O$ and −204.8 to −164.8‰ for δD. The deuterium excess is 7.2‰ (**Supplementary Table S2**) (Streletskaya et al., 2011). Ice mineralization in Late Pleistocene IW varies from 57 mg/L to 266 mg/L. Methane mean concentration in Pleistocene IW is 55 ppmV (0.06 ml/kg) (Streletskaya et al., 2018).

Dark gray clays (Unit 3) are underlain the section and have a visible thickness from 2 to 30 m. The sediments are saline (salinity up to 1.5%) and are classified as marine by the composition of water-soluble salts. The amount of the TOC in the clay deposits is 0.8–1.0%. The Wt% of clays varies along the section from 30–53 to 130%. Along the section, MTGI 35 m thick is exposed. The lower boundary of the ice layer is below the sea level. The MTGI represents frequent alternation of pure ice layers and relatively ice-rich soil. Inside the ice-soil layer large irregular mineral blocks of 0.4–1.0 m by 0.1–0.4 m^2 are present. Blocks contain dark gray clay with inclusions of pebbles and boulders with a diameter up to 0.4 m. Mineralization of ice varies from 311 mg/L to 1,068 mg/L(**Supplementary Table S2**). Ion composition shows the prevalence of bicarbonate-ions. Among cations, sodium-ions dominate, with concentrations increasing towards the center of MTGI. Stable isotope content in ice is rather constant and is −23‰ for oxygen and −174‰ for deuterium. The deuterium excess is on average 5.8‰ (**Supplementary Table S2**). This MTGI is similar to the first type of MTGI exposed at Marre-Sale, but has smaller methane concentration with an average of 301 ppmV (0.33 ml/kg) (Streletskaya, 2018). The MTGI of second type has the same characteristics as MTGI (II) of the Marre-Sale section.

DISCUSSION

Cryolithology

Three major sedimentary units were determined. Grain size composition of the studied sediments and the boundaries between the identified sedimentary units summarized in **Figure 10**.

Marine clays deposits formed during MIS 6-4 were found in the lower parts of the sections in almost all of the studied sites and comprise the oldest sedimentary unit (Unit 3). The deposits are represented by heavy loams and clays with a reticular, incompletely reticulated, or massive cryogenic structure with few inclusions of boulders and pebbles. On average, the ice content of mineral interlayers of loamy deposits is 20–30%, the total ice content is 40–50%. The deposits include a faunal complex characteristic of the Arctic seas margins. Freezing of the clay strata began after the sea regression, accompanied by frost cracking and the formation of the lower epigenetic parts of ice wedges. The transition from subaquatic to subaerial conditions marked by strong iron oxidizing along the edges of block units in the upper part of the clay horizon. With an increase in depth, iron oxidizing becomes less intensive and is confined mainly to fractured zones. The size of mineral blocks increases with depth, and the ice content of deposits decreases, which indicates a slowing of the freezing rate. In some outcrops, for example the SK section, a sedimentation break is observed which is marked by the development of erosion processes. As a result, there was a partial removal of the upper part of the clay strata.

The marine clays of Unit 3 in the MS and SK sites includes massive accumulations of very ice-rich sediments or practically pure ice with a relatively small amount of mineral inclusions - massive tabular ground ice (MTGI). Plicative and disjunctive deformations are often observed in ice-rich formations. The transition from overlying clays to MTGI is emphasized by a change in the cryostruture of the deposits from layered to irregularly meshy and coarse-blocks (block size about 30 × 20 cm, lenses 0.5–1 cm thick). Heavy minerals of the sand fraction in clay impurities in the MTGI are distinguished by almost perfect sorting. This distribution of particles is typical for sediment formed in shallow sea or near-delta part of river involving longshore currents and wave processing. The most probable origin hypothesis of the MTGI bodies occurring in marine clays is injection. This assumption can explain many structural features, such as high thickness and length, the presence of plicative and disjunctive deformations, and a large number of mineral inclusions.

Loamy-clayey marine deposits of Unit 3 are overlain by horizons of unsorted alluvial-marine, lacustrine, slope deposits of various compositions accumulated during MIS 2–3 (Unit 2). In the KR section, brown-gray loams and clays with a comminuted structure and oxidized iron along the cracks, represent this unit. In the SK section, sediments of this age compose the second terrace of the Yenisei River and are represented by layered sandy loams and fine sands of 4–10 m thick. A well-preserved mammoth carcass was discovered in these sediments, the radiocarbon age of which was about 37–44 ka BP (Maschenko et al., 2017). Alluvial-lacustrine sediments include large syngenetic IW up to 10 m long and 3–4 m wide at the top. In the DI site, silty ice-rich deposits of the MIS 2 (Sartan age), containing thick ice wedges form a specific stratum of the Ice Complex ("yedoma"). The lower narrow ends of ice wedges penetrate into the Unit 3. The syngenetic nature of

accumulation and freezing is indicated by the layering of the deposits, which is emphasized by the belt cryogenic structure. Ice-rich deposits often have a microscale cryogenic structure with vertically oriented lenses and a total ice content of 30–55%. Less icy sandy deposits are characterized by a massive cryostructure with a total ice content of 15–20%. Sandy ice-rich sediments in the MS section contain lenses and interlayers of pure glassy ice. This horizon is classified as Type 1 of MTGI. The horizon is an alternation of sub-horizontal (dislocated) layers of ice from a few centimeters to 1.5 m thick in sandy, sandy loam deposits.

Alluvial, alluvial-marine, lacustrine, and slope deposits of Unit 2 in all sections are overlain by a horizon of sandy, sandy loam alluvial, lacustrine, aeolian, deluvial deposits, or by peat of Holocene age (Unit 1). Cryostructure of sandy loams and sands are mainly massive, as well as semi-layered or oblique, consistent with sedimentary bedding. Ice content varies from 15% in sands to 70–80% in silty syngenetic sediments. The silty sandy loam and sandy deposits of Unit 1 are enveloping, for example, as in the MS and KR sections. Often, deposits of Unit 1 occur locally as inserts in earlier deposits, such as the lacustrine deposits in the PS site and in the southern part of the SK site. The Unit 1 deposits contains the complex of ice wedges. In the DI site, silty syngenetic sediments of the Holocene age are similar with composition, cryostructure, and other features to the underlying Pleistocene deposits. In the PS site, the embedding of Holocene lacustrine sediments with a thickness of 4–6 m and visible length of about 1,200 m was investigated. The lens consists of sandy loam saturated with organic matter. With increasing depth, light sandy loams turn into heavy sandy loams, the amount of organic content decreases, the content of silt particles increases from 35% at 1.4 m depth to 56% 3.7 m depth. Ice content increases with depth from 33% at 1.4 m depth to 65% 3.2 m depth. The cryostructure of sandy loam is layered. Lacustrine sandy loam transforms into silty sandy loam, characterized by a fine-mesh post-cryogenic structure (during thawing the sediments crumbles into small pieces). These deposits characteristic of the talik formed under lake.

Geochronology and Stratigraphy

Results of radiocarbon dating showed the formation of ice wedges occurred from more than 47 ka BP near Sopochnaya Karga Cape to about 3.6 ka BP on Sibiryakov Island (**Supplementary Table S1**). The stratification of ice rich sequences varies from site to site (**Figures 2–9**). In some cases, the ice-rich continental sediments cover ice-rich marine sediments with MTGI dated over 70 ka BP (Molodkov and Bolikhovskaya, 2009). The key outcrops have similar structure in terms of the sequence of lithological complexes, the change in the genesis and age of the enclosing sediments and the presence of organic material. Part of the sections of the Late Pleistocene - Holocene lies directly on the bedrock of the folded complex of Taimyr (DI), while the main part of the reference sections lies on the Cenozoic sedimentary rock material of the West Siberian basin.

The geochronological referencing of the studied complexes to local stratigraphic subdivisions (units) of Western Siberia was made based on the most typical to the region Kazantsevo horizon (MIS 5), the stratotypes of which are reliably dated along the Yenisei River to the south of the study area (Gusev et al., 2016), as well as at the study area (Streletskaya et al., 2007). At the base of the coastal cliffs of the Yenisei, Yenisei Gulf, Yamal and Gydanskaya Bay, basement loams of the Middle and Late Pleistocene are often exposed, which sometimes include thick MTGI. Ice wedges are usually found stratigraphically higher, in MIS 3 – MIS 1 sediments. Holocene sediments containing IW are discoveres in all key sites. The filling of thermokarst depression in some sections (EM, PS, SK) occurred in two stages. Deposits accumulated during the first stage in the beginning of the Holocene. They got into the lake during the destruction of coasts formed by dusty sandy silts with high ice content. Peat accumulates in the second stage of filling depressions. Holocene organic and peat-bearing sediments, accumulating mainly from the Early Holocene, top the section but in some places these settings persisted throughout the Holocene.

Geochemical Study of Ground Ice

Late Pleistocene IW and enclosing sediments have mineralization of ice from 25 to 266 mg/L with prevailing hydrocarbonate and calcium ions. The chloride content does not exceed 30% in the DI and MS areas, its content in IW of other key sites is much lower (in EM – 10%; in SK – 16%). Holocene IW and enclosing sediments is also have low salinity. Mineralization of ice is 17–360 mg/L with prevailing hydrocarbonate, chloride and sodium ions. The chloride content exceeds 30%, and it reaches 50% among the anions in the DI, SB and MS sections. The exception is Holocene IW of the EM section where the chloride content does not exceed several percent. The low mineralization and the predominance of hydrocarbonates most likely indicate the atmospheric nature of the water which formed IW in the Late Pleistocene and Holocene.

For chlorides, a direct correlation was established between the concentrations of ions in the snow cover with the average and total concentrations in atmospheric precipitation over the period of the snow cover occurrence. Forming over the sea surface, winter precipitation can contain sea salts, which are transported over large distances. The chemical composition of ice in Holocene and modern ice wedges (MS, SB, and DI) is dominated by the "marine" elements (Cl and Na), which reflects the closer position of the coastline (Kotov, 1991; Streletskaya and Vasiliev, 2009; Vasil'chuk, 2016). Winter precipitation was formed in the continental conditions, when the land occupied the modern shelf during the last cold stage (MIS 2) to 120 m depth. Domination of chloride and sodium ions in chemical composition of Late Pleistocene IW determines the increasing proximity of the sea in the Holocene. The large variability in mineralization and ion content in Holocene IW is determined by the dynamics of the sea ice cover. At EM, MA, PS, SK sections the amount of chloride in ice wedges is less owing to the preservation of ice in the Yenisei Bay and Gydan Bay in summer. In glacial cores of the ice field of the Nordaustlandet (Svalbard) and Vavilov glacier (Severnaya Zemlya), variations of the main «sea» components in the ice content correlate in time with the dynamics of the sea ice cover (Korzun, 1985).

The chemical composition of MTGI reflects the composition of groundwater before freezing (Anisimova, 1981; Streletskaya and Leibman, 2003; Vasil'chuk, 2016; Ivanova, 2012).

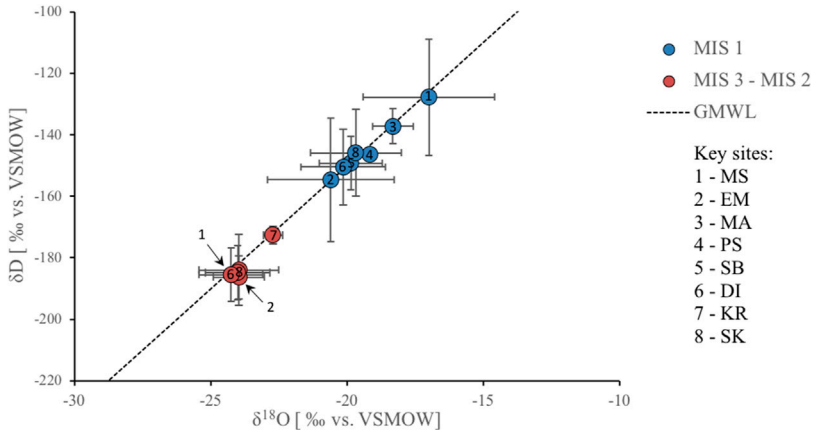

FIGURE 11 | Compilation of stable isotope data (δ ^{18}O, δ D) in Late Pleistocene and Holocene generations of syngenetic ice wedges (IW) exposed at the Kara Sea. Ice-wedge data sources: Holocene (MIS 1) and Late Pleistocene (MIS 2–3) (see **Supplementary Table S1**). Data are shown with respect to the Global Meteoric Water Line (GMWL) (Craig, 1961).

Mineralization of MTGI of both types varies from 23 to 1,068 mg/L and depends on the degree of "pollution" of the formation ice with mineral inclusions, but mostly determined by a mechanism of MTGI formation. Mineralization in MTGI of first type depends on the amount of mineral admixture in the ice: less and more mineralized interlayers alternate. Mineralization in MTGI of second type increases with depth, sodium predominates among cations, and its content increases to 92% with depth. In all samples, the sodium ion predominates among the anions. An increase in mineralization with depth is typical for freezing of closed talik systems (Anisimova, 1981). Mineralization of MTGI is in a wide range, but the composition of the salts dominated by sodium chloride. The results of geochemical analysis make it possible to confirm the subsoil conditions for the MTGI formation (MS and SK).

Methane in Frozen Sediments and Ground Ice

The methane content in ground ice and frozen sediments has been studied in the Marre-Sale and Sopochnaya Karga sections. Detailed characteristics of methane concentration were provided in previous works (Streletskaya et al., 2018; Oblogov et al., 2020). Sediment type have a strong influence on the methane concentration in permafrost. The highest methane concentrations are characteristic for marine clays of the Pre-Kargino time (MIS 3 and older). Here, the methane content averages 3,875 ± 3,468 ppmv (mean ± standard deviation), the minimum methane content is typical for sandy sediments of MIS 2 – MIS 1 - 195 ± 265 ppmv. Thus, despite the high variability, the methane content can serve as an indicator of the formation conditions of deposits and can be useful as an indicator for the geological and geocryological classification. The methane content in IW also differs depending on their age. In the Holocene IW, the methane content of 146 ± 241 ppmv is higher than in Late Pleistocene IW of 40 ± 82 ppmv. Large difference in the methane content in IW can also be useful to estimate the IW age. The MTGI represents a high methane content - up to 1,500 ± 2,400 ppmv. For instance, the methane content in the MTGI is about 100–1,000 times higher than in the ice sheets of Antarctica and Greenland (Raynaud, 2012). This confirms the non-atmospheric, subsoil genesis of the MTGI.

Stable-Isotope Composition of Ground Ice

Ice wedges have been widely used to reconstruct winter climate conditions across Siberia at glacial/interglacial timescales (Vasil'chuk, 1992; Streletskaya et al., 2013; Meyer et al., 2015; Streletskaya et al., 2015; Opel et al., 2017; Porter and Opel, 2020). Stable isotope compositions for different generations of ice wedges were analyzed for a reconstruction of the palaeoclimate environment. The stable isotope variations of relict ice wedges are used for qualitative inferences of winter temperature. It is given for ice wedges of nine geocryological sections. The isotopic composition of ice wedges on Kara Sea coasts is highly variable throughout time, ranging between −27‰ and −11‰ for δ^{18}O and from −208‰ to −90‰ for δD. We have observed a relatively constant stable isotopic composition within a single IW. For all ice wedges including recent ice wedges, the mean d_{excess} varies between 5 and 12‰. Recent ice wedges, sampled in the active layer have heavier isotopic compositions around −17.0‰ for δ^{18}O and −121.0‰ for δD (Streletskaya et al., 2011).

The Holocene ice wedges characterized by relatively heavy isotopic composition. The ice wedges of the Pakha-Sale Cape, Gydan Bay show a mean isotopic composition around −20.4‰ for δ^{18}O and −154.2‰ for δD. The ice wedges of the Dikson and Sopochnaya Karga show a same isotopic composition around −20.6‰ for δ^{18}O and −154.0‰ for δD (**Figure 11**).

The accuracy of paleotemperature estimates based on isotope trends in relict ground ice depends on the assumptions that the precipitation seasonality of relict ice and the relationship between

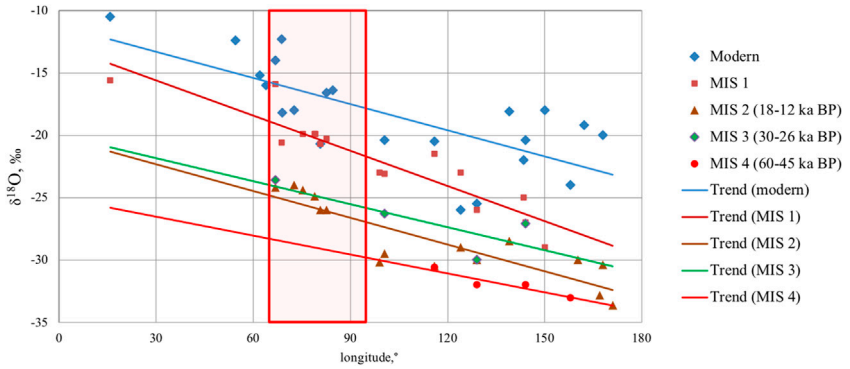

FIGURE 12 | Spatial distributions of oxygen stable isotopes $\delta^{18}O$, ‰ and their trend lines in ice-wedges-formed at different times in the Russian Arctic (after Streletskaya et al. (2015)). The study area is marked with a red rectangle.

precipitation-isotope ratios and air temperatures were constant. Ice-rich permafrost can be very resilient and survive even several interglacials (Wetterich et al., 2019).

Non temperature-related effects in the isotope record under the land–ocean configuration (e.g., sea level, ice sheet topography) which was different from today with possible differences in moisture source and trajectory of moist air parcels were previously discussed (Jouzel, 1999). We have summarized mean ice-wedge $\delta^{18}O$ data across the northern high latitudes for several periods: MIS 3 (30–26 ka BP), MIS 2 (18–12 ka BP), Holocene (last 12 ka BP), and modern (last several decades) in order to examine broad spatial and temporal patterns.

Temperature estimates (Vasil'chuk, 1992) show that average January temperature in the Dikson area dropped to −40 ± 3°C during Late Pleistocene IW formation. This is approximately 12–15° lower than the average January air temperatures (according to the Dikson meteorological station, the average January temperature is −25.5°C). Calculation of the average January air temperature using the same equation (Vasil'chuk, 1992) showed that for the Taimyr central regions (Cape Sabler), winter temperatures 18,000 years were the same or slightly lower (Derevyagin et al., 1999). The isotopic composition of the Late Pleistocene – Holocene IW in western Taimyr is close to the isotopic composition of IW on the Laptev and East Siberian coasts (Magens, 2005; Romanenko et al., 2011).

The isotopic composition of Holocene ice wedges reflects a higher temperature in winter and the influence of the sea. Active cracking and growth of syngenetic IW are associated with dry winters in the Holocene. Holocene ice wedges are heavier than older ones by an average of 6 ppm in oxygen isotope content depending on the location.

The similarity of ice formation conditions from Taimyr to Alaska makes it possible to use isotope data as correlation markers (Romanenko et al., 2011). The number of stable oxygen isotopes in Late Pleistocene ice wedges decreases from west to east (**Figure 12**) by 1–2‰; we observe the same reduction of isotopic composition in Holocene ice. The isotopic composition of ice wedges in the Late Pleistocene deposits, formed 12–25 ka BP, varies along the meridian in a narrow range. The direction of atmospheric transport from west to east has remained unchanged since the end of the Pleistocene.

Syngenetic IW with similar isotope content grew on Sverdrup Island and other Arctic islands (Tarasov et al., 1995, Romanenko et al., 2011). Severe winters at the time of ice formation are reconstructed based on the light isotopic composition of ice. The evidence of the hard continental conditions at the end of the Pleistocene on the Kara Sea shelf is the existence of relict subsea permafrost.

The content of stable oxygen isotopes in the MTGI of first type ($\delta^{18}O$) varies from −22 to −17‰ and for δD from −165.2 to −129‰. Deuterium excess changes from 5 to 10‰. Ice soils at the contact of the continental and marine units of the Marre-Sale sediments lay on the Global Meteoric Water Line (GLMW) along with data on ice wedges. The values of oxygen isotopes in the MTGI (SK) do not change extremely along the section and average −23‰, the values of d_{exc} are from 2 to 9‰. Thus, the MTGI of type I formation can be explained by the freezing of meteoric waters in an open system.

The MTGI of second type overlain by marine saline deposits have isotopic values that do not fall on the GMWL; their distribution is described by a line with a slope far from 8, which apparently indicates freezing of the initial waters in a closed system. The values of stable isotopes in the ice (MS) $\delta^{18}O$ varies from −22 to −7.5‰ and for δD - from −164‰ to −68‰. Deuterium excess varies from −1 to 12‰. With depth, isotopic compositions of ice becomes lighter. Values of the d_{exc} less than 10‰ are typical for ice formed during freezing of groundwater, or for surface water subjected to evaporative fractionation. The results of the isotopic composition in MTGI of second type support the in-ground conditions if ice formation.

CONCLUSION

Eight reference sections containing ground ice were investigated in the north of Western Siberia. The upper part of the Quaternary section in the north of Western Siberia can be attributed to ice-rich permafrost. The total ice content of the upper part of the section due to segregation ice, IW and MTGI

can reach 40–50%. In the lower part of the section, the ice content decreases to 30%.

The most typical section of Quaternary deposits was represented by the two-layered strata. The upper part of the section consists of continental sandy and sandy loam deposits formed during MIS 2 – MIS 1 (Sartan time and Holocene). Below this section, marine and coastal-marine sandy-loamy and clayey deposits formed during MIS 3 – MIS 5 (Kargino and Pre-Kargino times). Ice wedges were forming during MIS 3 – MIS 1 periods (Kargino, Sartan and Holocene horizons of the section). MTGI occurs at the border of the MIS 3 – MIS 2 horizon and Pre-Kargino horizons, as well as within the Pre-Kargino clay deposits.

In contrast to the Ice Complex of Eastern Siberia (Schirrmeister et al., 2011), the formation of ice rich permafrost in the Kara Sea coast occurred in two stages: marine stage with characteristic marine and coastal conditions (MIS 5 – MIS 3) and continental stage (MIS 3 – MIS 2). The MIS 3 – MIS 2 regression was accompanied by rapid cooling, dry climate and generation of syngenetic IW on the land and drained shelf area. The shelf of the Kara Sea was drained to the 110–120 m isobath (Stein et al., 2002) and the coastline retreated hundreds of kilometers north of its present position. At the same time epigenetic freezing of marine and coastal-marine sediments and MTGI formation occurred. The Holocene transgression of the Kara Sea proceeded unevenly with some fluctuations in the rate of sea level rise (Gornitz, 2009). During the climatic optimum of the Holocene degradation of the Late Pleistocene ice wedges occurred at the Kara Sea coast and caused erosion and slope processes. After thawing of the Pleistocene PWI ice ground-wedge casts were formed. Subsequent cooling in the Late Holocene caused freezing and formation of new generation of IW. The Holocene ice wedges are smaller in size and formed under more warmer climatic conditions than in Late Pleistocene.

Ground ice is a paleoenviromental archive that allows to establish sedimentation and ground ice formation at the end of the Late Pleistocene - Holocene. Base on isotopic composition of IW it was established that from MIS 4 to the present western atmospheric transport dominated in the Russian Western Arctic. There is a pronounced geographic trend in the isotopic composition of ice with highest $\delta^{18}O$ values found in the western and lowest values in the eastern part of the study region. Based on isotopic composition of ice wedges, winter air temperatures in MIS 3 – MIS 2 were 10–15°C lower than modern ones.

The chemical composition of IW is determined by the chemical composition of winter atmospheric precipitation and possible geochemical changes in the IW upper parts during the permafrost degradation. The presence of a strong "marine signal" with a high sodium chloride content in the Holocene IW may indicate the proximity of the sea during the IW formation and, in contrast, the remoteness of the sea during the Late Pleistocene IW formation.

High methane content in permafrost sediments is inherent in clayey sediments of marine origin; in continental sediments, the methane content is substantially lower. Thus, the methane content can also be used as an indicator for evaluation the genesis of sediments. The methane content in MTGI is 100–1,000 times higher than in glacial ice. This confirms the non-glacial genesis of the MTGI.

DATA AVAILABILITY STATEMENT

The original contributions presented in the study are included in the article/**Supplementary Material**, further inquiries can be directed to the corresponding author.

AUTHOR CONTRIBUTIONS

All authors contributed in data collection, processing, interpretation, and writing the manuscript.

FUNDING

This work is supported by State Scientific Program # 121041600043-4 and Research Program GM 1.5 «The cryosphere evolution under climate change and anthropogenic impact» No 121051100164-0.

ACKNOWLEDGMENTS

We sincerely thank P.B. Semenov and B.G. Vanshtein from VNIIokeangeologia (Saint Petersburg, Russia) who made quality control of the samples; Elizaveta Rivkina who determined concentration of methane in the Institute of Physical, Chemical, and Biological Problems in Soil Science RAS (Pushchino, Moscow Region, Russia); and Hanno Meyer who analyzed the isotope composition of ground ice in Isotope Laboratory of the Alfred Wegener Institute for Polar and Marine Research (Potsdam, Germany).

SUPPLEMENTARY MATERIAL

The Supplementary Material for this article can be found online at: https://www.frontiersin.org/articles/10.3389/feart.2021.723382/full#supplementary-material

REFERENCES

Alperin, M. J., and Reeburgh, W. S. (1985). Inhibition Experiments on Anaerobic Methane Oxidation. *Appl. Environ. Microbiol.* 50, 940–945. doi:10.1128/aem.50.4.940-945.1985

Anisimova, N. P. (1981). *Cryohydrogeochemistry of the Frozen Zone*. Novosibirsk: Nauka.

Astakhov, V. I. (2009). The Mid- and Late Neopleistocene of the Glacial Zone of Western Siberia: Problems in Stratigraphy and Paleogeography. *Bull. Comm. Quat. Period.* 69, 8–24.

Bolikhovsky, V. F. (1987). "Edoma Sediments of Western Siberia," in *New Data on the Geochronology of the Quaternary Period* (Moscow: Nauka).

Bolshiyanov, D. Yu., Makarov, A. S., Gusev, E. A., and Schneider, W. (2008). Problems of Ice Complex Origination and Former "Sannikovs Lands" Existence in the Laptev Sea. *Problemy Arktiki i Antarktiki.* 1, 151–160.

Craig, H. (1961). Isotopic Variations in Meteoric Waters. *Science.* 133, 1702–1703. doi:10.1126/science.133.3465.1702

Danilov, I. D. (1978). *Pleistocene of marine Subarctic plains*. Moscow: Moscow University Press.

Derevyagin, A. Y., Chizhov, A. B., Brezgunov, V. S., Hubberten, H. W., and Siegert, C. (1999). Isotopic Composition of Ice Wedges on Cape Sabler (Taimyr Lake). *Kriosfera Zemli.* 3, 41–49.

Dvornikov, Y. A., Leibman, M. O., Khomutov, A. V., Kizyakov, A. I., Semenov, P., Bussmann, I., et al. (2019). Gas-Emission Craters of the Yamal and Gydan Peninsulas: A Proposed Mechanism for lake Genesis and Development of Permafrost Landscapes. *Permafrost and Periglac Process.* 30, 146–162. doi:10.1002/ppp.2014

Forman, S. L., Ingólfsson, Ó., Gataullin, V., Manley, W., and Lokrantz, H. (2002). Late Quaternary Stratigraphy, Glacial Limits, and Paleoenvironments of the Marresale Area, Western Yamal Peninsula, Russia. *Quat. Res.* 57, 355–370. doi:10.1006/qres.2002.2322

Gataullin, V. N. (1988). *Upper Quaternary Deposits of the Western Coast of the Yamal Peninsula, Russia. [PhD Thesis Abstract]*. St. Petersburg: Federal Geological Institute.

Gornitz, V. (2009). "Sea Level Change, Post-Glacial," in *Encyclopedia of Paleoclimatology and Ancient Environments* (Dordrech: Springer).

Gusev, E. A., Anikina, N. Y., Arslanov, K. A., Bondarenko, S. A., Derevyanko, L. G., Molodkov, A. N., et al. (2013). Quaternary Deposits and Paleogeography of Sibiryakov Island During the Past 50 000. *Izvestija Russkogo Geograficheskogo Obcshestva.* 145 (4), 65–79.

Gusev, E. A., Molodkov, A. N., Streletskaya, I. D., Vasiliev, A. A., Anikina, N. Y., Bondarenko, S. A., et al. (2016). Deposits of the Kazantsevo Transgression (MIS 5) in the Northern Yenisei Region. *Russ. Geology. Geophys.* 57 (4), 586–596. doi:10.1016/j.rgg.2015.05.013

Gusev, E. A., Arslanov, H. A., Maksimov, F. E., Molodkov, A. N., Kuznetsov, V. Yu., Smirnov, S. B., et al. (2011). New Geochronological Data on NeoPleistocene - Holocene Sediments From Lower Yenisey Area. *Problemy Arktiki i Antarktiki.* 2, 36–44.

Ivanova, V. V. (2012). Geochemical Features of Formation of Massive Ground Ice Bodies (New Siberia Islands, Siberian Arctic) as the Evidence of Their Genesis. *Kriosfera Zemli.* 6 (1), 56–70.

Jouzel, J. (1999). Calibrating the Isotopic Paleothermometer. *Science.* 286 (5441), 910–911. doi:10.1126/science.286.5441.910

Kanevskiy, M., Shur, Y., Fortier, D., Jorgenson, M. T., and Stephani, E. (2011). Cryostratigraphy of Late Pleistocene Syngenetic Permafrost (Yedoma) in Northern Alaska, Itkillik River Exposure. *Quat. Res.* 75, 584–596. doi:10.1016/j.yqres2010.12.003

Kanevskiy, M. Z., Streletskaya, I. D., and Vasiliev, A. A. (2005). Regularities in the Formation of the Cryogenic Structure of the Quaternary Deposits of the Western Yamal (On the Example of the Marre-Sale District). *Earth's Cryosphere.* 9, 16–27.

Kaplanskaya, F. A., and Tarnogradskiy, V. D. (1986). Remnants of the Pleistocene Ice Sheets in the Permafrost Zone as an Object for Paleoglaciological Research. *Polar Geogr. Geology.* 10, 257–266. doi:10.1080/10889378609377295

Karpov, Y. G. (1986). *Ground Ice of the Yenissei North*. Novosibirsk: Nauka.

Korzun, A. V. (1985). *Geochemical Processes in Glacial and Underground Ice in Northern Eurasia [phd. Thesis]*. Moscow: MSU.

Kotov, A. N. (1991). "«Chemical Composition of Ice Wedges in Chukotka»," in *Comprehensive Geocryological Investigations of Chukotka*. Editor M. I. Tishin (Magadan: SEKNII DVO AN SSSR), 39–48.

Kritsuk, L. N. (2010). *Ground Ice of Western Siberia*. Moscow: Nauchnij mir.

Mackay, J. R. (1974). Ice-Wedge Cracks, Garry Island, Northwest Territories. *Can. J. Earth Sci.* 11, 1366–1383. doi:10.1139/e74-133

Magens, D. (2005). *Late Quaternary Climate and Environmental History of Siberian Arctic – Permafrost Records from Cape Mamontovy Klyk, Laptev Sea. [diplom Thesis]. [Kiel]*. Kiel: University of Kiel.

Maschenko, E. N., Potapova, O. R., Vershinina, A., Shapiro, B., Streletskaya, I. D., Vasiliev, A. A., et al. (2017). The Zhenya Mammoth (Mammuthus Primigenius (Blum.)): Taphonomy, Geology, Age, Morphology and Ancient DNA of a 48,000 Year Old Frozen Mummy From Western Taimyr, Russia. *Quat. Int.* 445, 104–134. doi:10.1016/j.quaint.2017.06.055

Meyer, H., Opel, T., Laepple, T., Dereviagin, A. Y., Hoffmann, K., and Werner, M. (2015). Long-Term Winter Warming Trend in the Siberian Arctic During the Mid- to Late Holocene. *Nat. Geosci.* 8 (2), 122–125. doi:10.1038/ngeo2349

Meyer, H., Schönicke, L., Wand, U., Hubberten, H. W., and Friedrichsen, H. (2000). Isotope Studies of Hydrogen and Oxygen in Ground Ice - Experiences With the Equilibration Technique. *Isotopes Environ. Health Stud.* 36, 133–149. doi:10.1080/10256010008032939

Michel, F. A. (1990). Isotopic Composition of Ice-Wedge Ice in Northwestern Canada. *Nordicana.* 54, 1–9.

Molodkov, A., and Bolikhovskaya, N. (2009). Climate Change Dynamics in Northern Eurasia Over the Last 200ka: Evidence From Mollusc-Based ESR-Chronostratigraphy and Vegetation Successions of the Loess-Palaeosol Records. *Quat. Int.* 201, 67–76. doi:10.1016/j.quaint.2008.05.028

Nikolayev, V. I., and Mikhalev, D. V. (1995). An Oxygen-Isotope Paleothermometer from Ice in Siberian Permafrost. *Quat. Res.* 43 (1), 14–21. doi:10.1006/qres.1995.1002

Oblogov, G. E. (2016). *Evolution of the Permafrost Zone of the Coast and Shelf of the Kara Sea in the Late Neopleistocene – Holocene. [phd. thesis]*. Tyumen: Earth Cryosphere Institute.

Oblogov, G. E., Streletskaya, I. D., Vasiliev, A. A., Gusev, E. A., and Arslanov, H. A. (2012). Quaternary Deposits and Geocryological Conditions of Gydan Bay Coast of the Kara Sea. *Tenth Int. Conf. Permafrost.* 3, 293–297.

Oblogov, G. E., Vasiliev, A. A., Streletskaya, I. D., Zadorozhnaya, N. A., Kuznetsova, A. O., Kanevskiy, M. Z., et al. (2020). Methane Content and Emission in the Permafrost Landscapes of Western Yamal, Russian Arctic. *Geosciences.* 10 (10), 412–421. doi:10.3390/geosciences10100412

Okhotin, V. V. (1933). *Granulometric Classification of Soils Based on Their Physical and Mechanical Properties*. Leningrad: Lengostransizdat.

Opel, T., Wetterich, S., Meyer, H., Dereviagin, A. Y., Fuchs, M. C., and Schirrmeister, L. (2017). Ground-ice Stable Isotopes and Cryostratigraphy Reflect Late Quaternary Palaeoclimate in the Northeast Siberian Arctic (Oyogos Yar Coast, Dmitry Laptev Strait). *Clim. Past.* 13 (6), 587–611. doi:10.5194/cp-13-587-2017

Péwé, T. L., and Journaux, A. (1983). *Origin and Character of Loess-Like Silt in Unglaciated South-Central Yakutia, Siberia, USSR*. USGS Professional Paper. Washington, 1262, 1–45. doi:10.3133/pp1262

Pismeniuk, A., Streletskaya, I., and Gusev, E. (2019). "Quaternary Deposits of the Gydan peninsula Coast of Western Siberia and Their cryogenic Structure," in Abstracts of International Conference "Solving the puzzles from Cryosphere".

Podborny, E. E. (1978). "«The Time and Activity of thermal-contraction Cracks Formation»," in *Cryolitology Problems*. Editor A. I. Popov (Moscow: Moscow University Press), 132–140.

Popov, A. I. (1953). The peculiar Characteristics of the Lithogenesis of Alluvial plains in Severe Climatic Conditions. *Izvestiya Akademii Nauk SSSR, Geogr. Ser.* 2, 29–41.

Porter, T. J., and Opel, T. (2020). Recent Advances in Paleoclimatological Studies of Arctic Wedge- and Pore-ice Stable-Water Isotope Records. *Permafrost and Periglac Process.* 31 (31), 429–441. doi:10.1002/ppp.2052

Raynaud, D. (2012). The Integrity of the Ice Record of Greenhouse Gases With a Special Focus on Atmospheric CO_2. *Led. I Sneg.* 2 (118), 5–14

Romanenko, F. A., Nikolaev, V. I., and Arkhipov, V. V. (2011). Changes in the Isotope Composition of Ice Deposits of the East Siberian Sea Coast: Geographical Aspect. *Led i Sneg.* 1 (113), 93–104.

Romanovskiy, N. N. (1993). *Fundamentals of Cryogenesis of the Lithosphere*. Moscow: Moscow State University.

Schirrmeister, L., Grosse, G., Schwamborn, G., Andreev, A. A., Meyer, H., Kunitsky, V. V., et al. (2003). Late Quaternary History of the Accumulation plain north of the Chekanovsky Ridge (Lena Delta, Russia): a Multidisciplinary Approach. *Polar Geogr.* 27 (4), 277–319. doi:10.1080/789610225

Schirrmeister, L., Kunitsky, V., Grosse, G., Wetterich, S., Meyer, H., Schwamborn, G., et al. (2011). Sedimentary Characteristics and Origin of the Late Pleistocene Ice Complex on north-east Siberian Arctic Coastal Lowlands and Islands - A Review. *Quat. Int.* 241, 3–25. doi:10.1016/j.quaint.2010.04.004

Semenov, P. B., Pismeniuk, A. A., Malyshev, S. A., Leibman, M. O., Streletskaya, I. D., Shatrova, E. V., et al. (2020). Methane and Dissolved Organic Matter in the Ground Ice Samples from Central Yamal: Implications to Biogeochemical Cycling and Greenhouse Gas Emission. *Geosciences.* 10 (11), 450. doi:10.3390/geosciences10110450

Slagoda, E. A., Opokina, O. L., Rogov, V. V., and Kurchatova, A. N. (2012). Structure and Genesis of Underground Ice in Upper Pleistocene-Holocene Deposits of Cape Marre-Sale (Western Yamal). *Earth's Cryosphere.* 16 (2), 9–22.

Solomatin, V. I. (1982). «*Buried Ice, Patterns of Formation and Structure*», *in Layered Ice of the Permafrost Zone*. Yakutsk: IM SO AN SSSR, 97–104.

Stein, R., Niessen, F., Dittmers, K., Levitan, M., Schoster, F., Simstich, J., et al. (2002). Siberian River Run-Off and Late Quaternary Glaciation in the Southern Kara Sea, Arctic Ocean: Preliminary Results. *Polar Res.* 21 (2), 315–322. doi:10.3402/polar.v21i2.6493

Streletskaya, I. D., Gusev, E. A., Vasiliev, A. A., Kanevskiy, M. Z., Anikina, N. Yu., and Derevyanko, L. G. (2007). New Results of Quaternary Sediment Studies of Western Taymyr. *Earth's Cryosphere.* 6 (3), 14–28.

Streletskaya, I. D., Gusev, E. A., Vasiliev, A. A., Rekant, P. V., and Arslanov, Kh. A. (2012a). Late Pleistocene-Holocene Ground Ice in Quaternary Deposits on the Kara Shelf as a Record of Paleogeographic Conditions. *Bull. Comm. Quat. Period.* 72, 28–59.

Streletskaya, I. D., Vasiliev, A. A., Slagoda, E. A., Opokina, O. L., and Oblogov, G. E. (2012b). Ice Wedges on Sibiryakov Island (Kara Sea) Bulletin of Moscow University. *Ser. Geogr.* 3, 57–63.

Streletskaya, I. D., Kanevskiy, M. Z., and Vasiliev and, A. A. (2006). Massive Ground Ice in Dislocated Quaternary Sediments of Western Yamal. *Earth's Cryosphere.* 10, 68–78.

Streletskaya, I. D., and Leibman, M. O. (2003). "«Cryogeochemical Model of Tabular Ground Ice and Cryopegs Formation at Central Yamal, Russia»," in Proceedings of the Eighth International Conference on Permafrost 2. Editors M. Phillips, S. M. Springman, and L. U. Arenson (Lisse: Balkema), 1111–1115.

Streletskaya, I. D., Shpolyanskaya, N. A., Kritsuk, L. N., and Surkov, A. V. (2009). Cenozoic Deposits of the Western Yamal and the Problem of Their Genesis. Vestnik of the Moscow State University. *Ser. Geogr.* 3, 50–57.

Streletskaya, I. D., and Vasiliev, A. A. (2009). Isotopic Composition of Ice Wedges of West Taymir. *Earth's Cryosphere.* 8 (3), 59–69.

Streletskaya, I. D., Vasiliev, A. A., and Kanevskiy, M. Z. (2008). "«Freezing of marine Sediments and Formation of continental Permafrost at the Coasts of Yenisey Gulf»," in Proceedings of Ninth International Conference on Permafrost 2. Editors D. L. Kane and K. M. Hinkel (Fairbanks: Institute of Northern Engineering, University of Alaska Fairbanks), 1722–1726.

Streletskaya, I. D., Vasiliev, A. A., Oblogov, G. E., and Tokarev, I. V. (2015). Reconstruction of Paleoclimate of Russian Arctic in Late Pleistocene–Holocene on the Basis of Isotope Study of Ice Wedges. *Earth's Cryosphere.* 19 (2), 86–94.

Streletskaya, I., Gusev, E., Vasiliev, A., Oblogov, G., and Molodkov, A. (2013). Pleistocene-Holocene Palaeoenvironmental Records From Permafrost Sequences at the Kara Sea Coast (Nw Siberia, Russia). *Geogr. Environ. Sustain.* 6, 60–76. doi:10.24057/2071-9388-2013-6-3-60-76

Streletskaya, I., Vasiliev, A., and Meyer, H. (2011). Isotopic Composition of Syngenetic Ice Wedges and Palaeoclimatic Reconstruction, Western Taymyr, Russian Arctic. *Permafrost Periglac. Process.* 22, 101–106. doi:10.1002/ppp.707

Streletskaya, I., Vasiliev, A., Oblogov, G., and Streletskiy, D. (2018). Methane Content in Ground Ice and Sediments of the Kara Sea Coast. *Geosciences.* 8 (12), 434. doi:10.3390/geosciences8120434

Tarasov, P. E., Andreev, A. A., Romanenko, F. A., and Sulerzhitskii, L. D. (1995). Palynostratigraphy of Upper Quaternary Deposits of Sverdrup Island, the Kara Sea. *Stratigr. Geol. Correl.* 3, 190–196. doi:10.1016/0037-0738(94)00119-F

Tomirdiaro, S. V. (1980). *The Loess-Ice Formation of East Siberia in the Late Pleistocene*. Moscow: Nauka.

Vasil'chuk, Y. K. (1992). *Oxygen Isotope Composition of Ground Ice (Application to Paleogeocryological Reconstructions)*. Moscow: Geological Faculty of Moscow State University.

Vasil'chuk, Y. K. (2006). *Ice Wedge: Heterocyclity, Heterogeneity, Heterochroneity*. Moscow: Moscow University Press.

Vasil'chuk, Y. K. (2016). Geochemical Composition of Ground Ice of the Russian Arctic. *Arktika i Antarktika.* 2, 99–115. doi:10.7256/2453-8922.2016.2.21378

Wetterich, S., Rudaya, N., Kuznetsov, V., Maksimov, F., Opel, T., Meyer, H., et al. (2019). Ice Complex Formation on Bol'shoy Lyakhovsky Island (New Siberian Archipelago, East Siberian Arctic) Since about 200 Ka. *Quat. Res.* 92 (2), 530–548. doi:10.1017/qua.2019.6

Conflict of Interest: The authors declare that the research was conducted in the absence of any commercial or financial relationships that could be construed as a potential conflict of interest.

Publisher's Note: All claims expressed in this article are solely those of the authors and do not necessarily represent those of their affiliated organizations, or those of the publisher, the editors and the reviewers. Any product that may be evaluated in this article, or claim that may be made by its manufacturer, is not guaranteed or endorsed by the publisher.